The Bilayer Enhances Rhodopsin Kinetic Stability in Bovine Rod Outer Segment Disk Membranes

Scott C. Corley,[†] Peter Sprangers,[‡] and Arlene D. Albert[†*]
[†]Department of Molecular and Cell Biology, University of Connecticut, Storrs, Connecticut; and [‡]Department of Statistics, The Ohio State University, Columbus, Ohio

ABSTRACT Rhodopsin is a kinetically stable protein constituting >90% of rod outer segment disk membrane protein. To investigate the bilayer contribution to rhodopsin kinetic stability, disk membranes were systematically disrupted by octyl-β-D-glucopyranoside. Rhodopsin kinetic stability was examined under subsolubilizing (rhodopsin in a bilayer environment perturbed by octyl-β-D-glucopyranoside) and under fully solubilizing conditions (rhodopsin in a micelle with cosolubilized phospholipids). As determined by DSC, rhodopsin exhibited a scan-rate-dependent irreversible endothermic transition at all stages of solubilization. The transition temperature (T_m) decreased in the subsolubilizing stage. However, once the rhodopsin was in a micelle environment there was little change of the T_m as the phospholipid/rhodopsin ratio in the mixed micelles decreased during the fully solubilized stage. Rhodopsin thermal denaturation is consistent with the two-state irreversible model at all stages of solubilization. The activation energy of denaturation (E_{act}) was calculated from the scan rate dependence of the T_m and from the rate of rhodopsin thermal bleaching at all stages of solubilization. The E_{act} as determined by both techniques decreased in the subsolubilizing stage, but remained constant once fully solubilized. These results indicate the bilayer structure increases the E_{act} to rhodopsin denaturation.

INTRODUCTION

In recent years it has become clear that many proteins are kinetically stable. These proteins may or may not also exhibit thermodynamic stability (1). In the simplest case, the native, biologically active state of a kinetically stable protein need not be the thermodynamically favored state. However, the native state is protected from denaturation by an energy barrier. Although this energy barrier may inhibit the formation of the final denatured state, it may also function to reduce the occurrence of intermediate states that may be prone to aggregation (2–4). Additionally, it has been proposed that kinetic stabilization may allow functional properties to be optimized (5). Finally, because kinetically stable proteins exhibit a finite lifetime, this type of stability could serve as a timer for biological function (5–11). Several membrane proteins have been shown to undergo thermal denaturation in a kinetically controlled manner. We have shown both rhodopsin and opsin to be kinetically stable (12,13). Other examples include cytochrome *c* oxidase (14), bacteriorhodopsin (15), the GLUT 1 receptor (16), the sarcoplasmic reticulum Ca^{2+} ATPase (17,18), and erythrocyte ghost proteins (19).

Integral membrane proteins are imbedded in the matrix of the lipid bilayer. The membrane bilayer supports a complex interplay between the lipids and proteins that stabilizes the function and structure of the imbedded proteins. Many years ago it was observed that integral membrane proteins typically lose function once removed from the bilayer by detergent solubilization (20,21). However, the mechanism of membrane protein stabilization by the bilayer remained elusive. To further our understanding of the role of the bilayer environment, we have investigated the changes in the kinetic stability of rhodopsin as the native rod outer segment disk membrane is disrupted and finally completely solubilized by the nonionic detergent, octyl β-D-glucopyranoside (OG).

The rod outer segment disk membrane is particularly amenable to investigations of protein stabilization by the lipid bilayer and to investigations of protein-lipid interactions. The integral membrane protein of the disk membrane is greater than 90% rhodopsin (22). Therefore, biophysical measurements of the native disk membrane proteins overwhelmingly reflect rhodopsin properties in the native membrane environment. Furthermore, the photoreceptor rhodopsin exists in two forms that exhibit strikingly different stabilities. Therefore, two forms of the protein can be investigated. The dark-adapted form, rhodopsin has a bound chromophore, 11-*cis*-retinal. Opsin is the apoprotein and is formed upon exposure to light. It has long been recognized that rhodopsin exhibits greater thermal stability than opsin (23). Differential DSC has shown that rhodopsin has a T_m ~15°C higher than opsin (24–27) and a higher activation energy of denaturation (E_{act}) (12). When opsin and rhodopsin are present in the same membrane, the endothermic thermal transitions of the two forms do not affect one another indicating that opsin and rhodopsin behave as independent monomers before denaturation (13).

These studies are designed to demonstrate that the bilayer plays a critical role in the kinetic stability of rhodopsin/opsin. In this study, we systematically altered the environment of rhodopsin and opsin by disrupting the disk membrane using

Submitted November 1, 2010, and accepted for publication May 9, 2011.

*Correspondence: arlene.albert@uconn.edu

Editor: Heiko H. Heerklotz.

0006-3495/11/06/2946/9 $2.00

doi: 10.1016/j.bpj.2011.05.015

OG. This nonionic detergent was chosen because the mechanism of solubilization of the disk membrane by OG has been well characterized (21,28,29). Here, we show that as the membrane bilayer is disrupted, the E_{act} to rhodopsin and opsin thermal denaturation is dramatically lowered. However, no additional lowering of E_{act} is observed with further detergent addition once rhodopsin is in mixed micelles, regardless of the phospholipid/rhodopsin ratio in the micelles. These data indicate the intact bilayer is critical to the kinetic stability of rhodopsin and opsin.

MATERIALS AND METHODS

Preparation of disk membranes

Fresh bovine retinas were obtained from Lawson (Lincoln, NE). Rod outer segments (ROS) were isolated from bovine retinas as described (22). Osmotically intact disk membranes were isolated from ROS as described (30). Disks were washed at least twice in 10 mM potassium phosphate (KPO_4^-), pH 7.0, by centrifugation. Rhodopsin concentration was determined from the change in absorbance at 500 nm after photobleaching in the presence of 0.05 M hydroxylamine using the molar extinction coefficient of 40,000 $cm^{-1}M^{-1}$. All isolation was conducted under dim red light. Disks were bleached by exposure to continuous white light for 1 min.

Solubilization in octyl β-D-glucopyranoside

OG was purchased from Calbiochem (La Jolla, CA, Cat. No. 494459). Disk membrane aliquots were solubilized at concentrations of 5, 6.7, 10, 13.3, 20, 50, 75, 100, and 200 mM OG in 10 mM KPO_4^-, pH 7.0. The rhodopsin concentration was 1.5 mg/ml rhodopsin for all samples. Aliquots were stored at −80°C after solubilization.

DSC

DSC was performed using a MicroCal VP-DSC microcalorimeter (Northampton, MA). All buffers and samples were degassed (10 min, 20°C) in a MicroCal Thermovac. Samples were loaded under dim red light. Samples were heated from 20°C to 120°C at scan rates of 1.5°C/min, 1.0°C/min, 0.5°C/min, and 0.25°C/min. Two consecutive scans were recorded for each sample. The second scan was transitionless and used as a baseline for the first scan. Analysis of DSC data was conducted using MicroCal Origin 5.0 software. The T_m was determined from the maximum of each transition. The peak width at half height, $t_{1/2}$, was determined by Origin. The apparent calorimetric enthalpy (ΔH_{cal}) was determined by the integration of each transition peak from the baseline.

The E_{act} was determined from the scan rate dependence of the T_m using the following equation (31):

$$\ln(\text{scanning rate}/T_m^2) = \text{const} - \frac{E_{act}}{RT_m},$$

where T_m is the transition peak maxima and R is the universal gas constant.

The E_{act} was also determined at selected OG concentrations from its dependence on the peak height (C_p^{max}) relative to the area of the transition peak (Q_t) using the following equation (31):

$$E_{act} = eRC_p^{max}\frac{T_m}{Q_t}.$$

The fits of the data to the two-state irreversible model were carried out as described (2,32).

Thermal bleaching kinetics of rhodopsin

Rhodopsin thermal bleaching kinetics was examined using 20 μl aliquots (1.5 mg/ml) of rhodopsin at temperatures ranging from 5°C to 10°C below the temperature of thermal denaturation to 1–2°C above the T_m of thermal denaturation determined from DSC. For example, rhodopsin in the native disk membrane was heated to temperatures between 63°C and 74°C for 4–90 min. Aliquots were sequentially removed from heat at timed intervals. The concentration of rhodopsin that resisted thermal bleaching was determined from the change in absorbance at 500 nm after photobleaching in the presence of 0.05 M hydroxylamine using the molar extinction coefficient of 40,000 $cm^{-1}M^{-1}$. The E_{act} of thermal bleaching was determined from the Arrhenius expression:

$$\ln\frac{k_1}{k_2} = \frac{E_{act}}{R}\left(\frac{1}{T_2} - \frac{1}{T_1}\right),$$

where k_1 and k_2 are the velocity constants of thermal bleaching at absolute temperatures T_1 and T_2, and R is the universal gas constant.

Statistical analysis of E_{act} data

The data for E_{act} versus OG for E_{act} determined calorimetrically and E_{act} determined spectroscopically were analyzed in two subsets. The values above and below the 30 mM OG threshold were taken separately. Below 30 mM OG, the data were analyzed using ordinary least squares regression. To assess the colinearity of DSC E_{act} and spectroscopically determined E_{act}, an indicator variable process was added to a linear model already containing OG concentration. The statistical significance of this indicator variable shows whether or not the two processes generate different values of E_{act} given a value of OG.

Above the 30 mM OG threshold, we built another linear model predicting E_{act} from the value of OG and a variable indicating which process was used. The statistical significance of the slope coefficient for OG concentration indicates if OG concentration is an important predictor of E_{act}, or if E_{act} and OG concentration appear to be independent. Similar to the previous model, the indicator variable in our linear model shows whether or not the two processes generate different values of E_{act} given a value of OG.

Due to the paucity of data, we also compared the two processes using the Wilcoxon rank-sum test. The Wilcoxon test is the nonparametric analog of the two-sample t-test. If the p-value for the indicator variable in our linear model is similar to the p-value in the nonparametric test, we can be confident that our linear model is not in violation of its distributional assumptions.

RESULTS

Membrane disruption by octyl β-D-glucopyranoside

To determine the dependence of the kinetic stability of rhodopsin and opsin on the integrity of the disk lipid bilayer, it was important to disrupt the membrane in a well-defined manner. The stages of disk membrane solubilization by OG have been described in detail (21,33). Briefly, Stubbs and Litman demonstrated that solubilization proceeds in specific stages. In the first stage OG partitions into the bilayer and saturates it. Subsequent to detergent saturation, the bilayer fragments and mixed micelles of rhodopsin, phospholipids, and detergent are released. The final stage occurs when the detergent is above its critical micelle concentration, 20 mM (28,34). In this final stage rhodopsin, phospholipids, and detergent exist in mixed micelles in which the lipid may

or may not interact with rhodopsin. As the OG concentration is raised well beyond its critical micelle concentration , the ratio of phospholipid/rhodopsin in the detergent micelles decreases. In the studies presented here membrane disruption is divided into subsolubilized and solubilized stages.

Membrane disruption results in a decrease of the rhodopsin and opsin T_m

DSC was used to monitor the effects of detergent disruption of the native disk membrane bilayer on rhodopsin and opsin. Thermograms of ROS disks and solubilized disk membranes were obtained between 20°C and 120°C. This temperature range allowed the endothermic transition and an apparent exothermic transition of rhodopsin in disk membranes under subsolubilized and solubilized conditions to be observed. However, due to the coin-shaped cells in the VP-DSC (MicroCal) used for these experiments the exothermic transition may result from a change in sample viscosity upon protein aggregation. Therefore, this transition is not further analyzed in this study. The three thermograms shown in Fig. 1 represent critical points in disk membrane solubilization. Under our experimental conditions (1.5 mg/ml rhodopsin), at 20 mM OG the bilayer is saturated with OG and the membrane begins to fragment. At 100 mM OG, rhodopsin is predominately found in mixed micelles with a phospholipid/rhodopsin ratio of ~10:1. From these thermograms it is clear that the rhodopsin endothermic transition and the exothermic transition are sensitive to membrane disruption by OG.

The dependence of the T_m on the extent of membrane disruption was investigated at OG concentrations that correspond to subsolubilizing levels through complete solubilization of the disk membranes. As is typical for irreversible processes, the transitions are asymmetric. Therefore, in these studies T_m was determined at the maximum of the transition. Rhodopsin is a kinetically stable membrane protein and as such its transition temperature (T_m) is scan-rate dependent (12). Each T_m was determined at four different scan rates. The dependence of the T_m on the degree of solubilization is shown in Fig. 2 for each of the four scan rates. If these curves were fit to two straight lines they would intersect at ~30 mM OG. On the basis of the study by Stubbs and Litman (21), at a rhodopsin concentration of 1.5 mg/ml, 30 mM OG is sufficient to solubilize all of the disk membrane rhodopsin. Thus, this is the transition to the solubilized state in which rhodopsin exists entirely in mixed micelles with phospholipid and OG. At this point ~30 phospholipids/rhodopsin molecule are present with OG in a mixed micelle (21). Although this is a sufficient number of phospholipids to provide an annular ring around the protein, the arrangement of the phospholipids and rhodopsin within the micelle is unknown. Additional detergent generates mixed micelles containing rhodopsin with decreasing phospholipid content. At the highest concentration (200 mM OG) used in these experiments approximately four phospholipids were, on average, in the micelle with rhodopsin.

The effect of OG solubilization on opsin was also investigated. As shown in Fig. 2, at subsolubilizing OG concentrations the T_m of opsin decreases significantly with increasing OG concentration. However, in the time frame of our experiments, OG solubilized opsin denatures at room temperature (33). At ~20 mM OG the T_m approaches room temperature. Therefore, DSC studies at higher OG concentrations were not feasible.

Membrane disruption broadens the transition

We determined the width of each transition at one-half peak height. In Fig. 3 the width of the transition at one-half peak

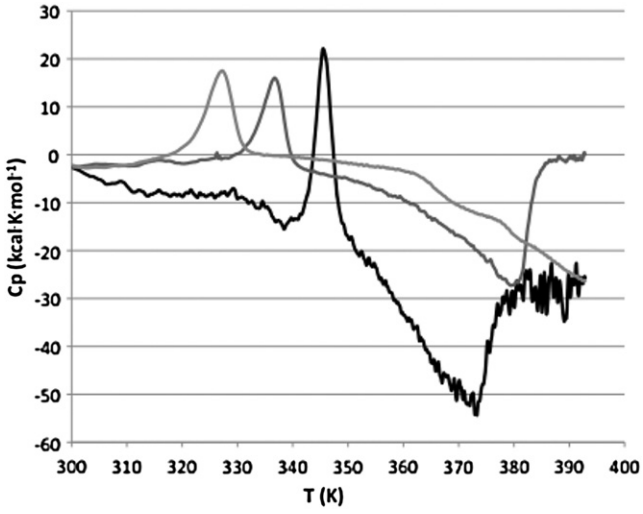

FIGURE 1 Thermograms of osmotically intact disk membranes (*black*) and of disks solubilized in OG at concentrations of 20 mM (*dark gray*) and 100 mM (*light gray*). The scan rate for each thermogram was 1.5 K/min.

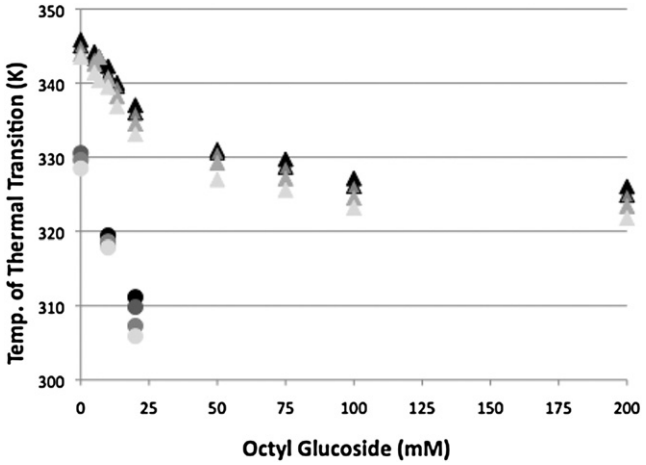

FIGURE 2 T_m of rhodopsin (*triangles*) and opsin (*circles*) thermal denaturation as a function of detergent concentration. The data were obtained at scan rates of 1.5 (*black*), 1.0 (*dark gray*), 0.5 (*gray*), and 0.25 (*light gray*) K/min.

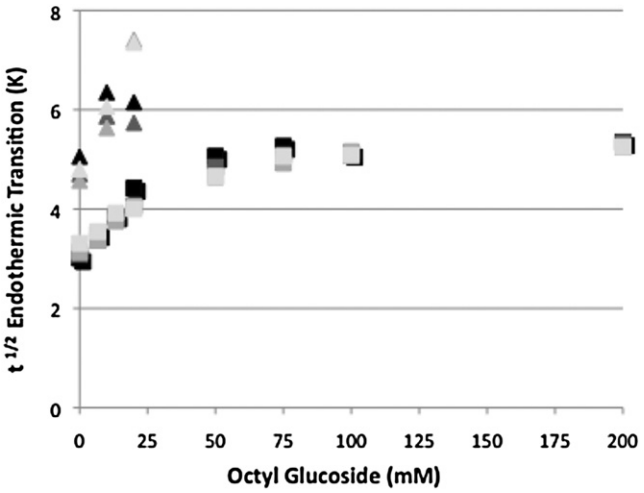

FIGURE 3 Peak width at half height ($t_{1/2}$) for rhodopsin (*squares*) and opsin (*triangles*) thermal denaturation at each detergent concentration. The were obtained at scan rates of 1.5 (*black*), 1.0 (*dark gray*), 0.5 (*gray*), and 0.25 K/min (*light gray*) K/min.

height of the rhodopsin transition increases significantly as detergent partitions into the bilayer and then remains essentially constant after rhodopsin is fully solubilized. As in Fig. 2, if this curve is fit with two straight lines, they intersect at ~30 mM OG. The width of the transition at one-half peak height of the opsin transition also increases significantly as detergent partitions into the bilayer. However, as described earlier opsin could not be investigated at solubilizing concentrations of OG.

The calorimetric enthalpy (ΔH_{cal}), the area under the transition curve is the heat measured for the transition. We did not observe any significant change in ΔH_{cal} with increasing detergent concentration (data not shown). That is, the heat absorbed during the endothermic phase of thermal denaturation appears to be independent of bilayer disruption.

Membrane disruption results in a decrease in rhodopsin and opsin E_{act} of thermal denaturation

The thermal denaturation of rhodopsin is irreversible. The Lumry-Erying model (35) has been used to describe the irreversible thermal denaturation of rhodopsin and opsin (12,13). In this model the native protein is in equilibrium with an unfolded specie(s) that can then undergo an irreversible denaturation:

$$N \Leftrightarrow U \Rightarrow D.$$

The consequences of this model have been discussed in detail elsewhere (1,4). Briefly, in a very simple case, if the conversion of U to D is slow relative to the rate of U conversion back to N, the equilibrium will dominate before the thermal transition. That is, before the transition temperature the formation of D is negligible. In this case the thermal transition will be essentially independent of scan rate and equilibrium thermodynamics can be employed to investigate the equilibrium process. As shown in Fig. 2, the T_m of rhodopsin is scan-rate dependent, consistent with conversion to D before the T_m.

It is also possible that the N to U equilibrium dominates before the T_m, but the protein rapidly aggregates after the T_m is reached. In this case it would be expected that if the protein were heated to temperatures approaching, but lower than the T_m reversibility would be observed. To examine this possibility, disk membranes were heated to temperatures approaching the T_m then cooled and rescanned. Reversibility of the denaturation was not observed. This is consistent with earlier studies that showed rhodopsin irreversibly denatured at 55°C (36).

Finally, the Lumry-Erying model can be represented by the two-state irreversible model if the rate of U conversion to D, which is the irreversible step, is sufficiently rapid on the experimental time scale that the concentration of U is always very small. Thus, only N and D will be present in significant amounts. N to U conversion is rate limiting if the rate of formation of U to D is rapid relative to the rate of U conversion back to N. In this case significant formation of D will occur during the transition, before the T_m and the T_m will be dependent on the scan rate. This scan rate dependence of T_m is characteristic of protein thermal denaturation that is under kinetic control. This thermal denaturation may be described as a two-state irreversible transition that exhibits first-order kinetics if the experimental calorimetric data are in good agreement with the Arrhenius equation (1,4). The rhodopsin calorimetric transitions are consistent with this case. In Fig. 4 the DSC thermograms are superimposed on a fit to the two-state irreversible model determined as described by Rodriguez-Larrea et al. (32). Furthermore, the rate constant determined from the calorimetric data for a two-state irreversible process should be independent of scan rate (1,4). An Arrhenius plot (Fig. 5) shows that rate constants determined for rhodopsin in the native disk, at 20 mM OG and under solubilizing conditions (100 mM OG), are independent of scan rate. Therefore, the two-state irreversible model adequately describes the thermal denaturation of rhodopsin in the native disk and provides an excellent description of the thermal denaturation of rhodopsin in the presence of OG. This may reflect a more complex protein and lipid organization in the native membrane.

Equilibrium thermodynamic parameters cannot be derived from calorimetric data of kinetically controlled processes. However, calorimetric data can be used to calculate the activation energy of thermal denaturation (E_{act}). In this study, E_{act} was calculated from the scan rate dependence of the T_m (31). As described in the methods, E_{act} for the transitions were calculated from the slopes of the lines shown in Fig. 6. This method relies only on the scan rate dependence of the T_m. This was our primary method of calculating E_{act} because it was not observed to be sensitive to baseline determinations.

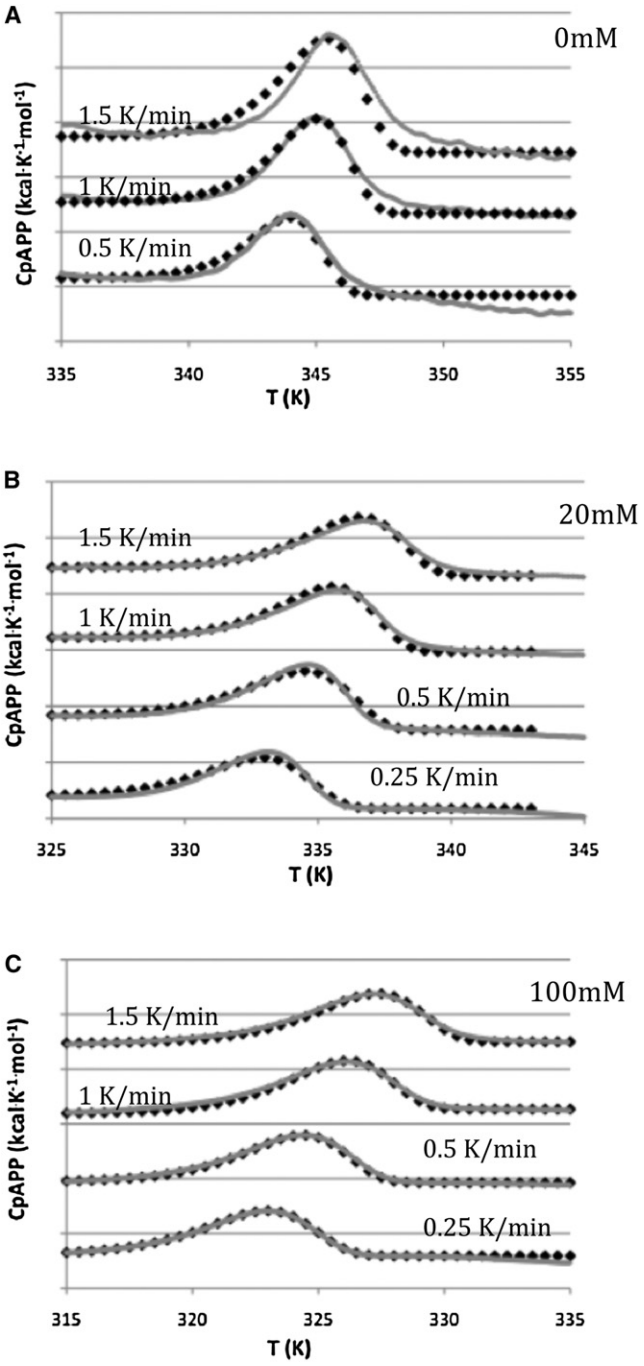

FIGURE 4 Comparison of experimental DSC thermograms of rhodopsin at the indicated scan rates (*continuous gray lines*) to calculations based on the two-state irreversible model (*black diamonds*). The thermograms have been staggered in the *y* axis for clarity. (*A*) Rhodopsin in intact disk membranes. (*B*) Rhodopsin in 20 mM OG. (*C*) Rhodopsin in 100 mM OG.

The dependence of E_{act} on the extent of membrane solubilization is shown in Fig. 7. Under subsolubilizing conditions, as OG partitions into the bilayer, the E_{act} of rhodopsin and opsin decrease in a similar manner. The E_{act} decreases from 160 kcal/mol to 100 kcal/mol for rhodopsin and from 120 kcal/mol to 60 kcal/mol for opsin

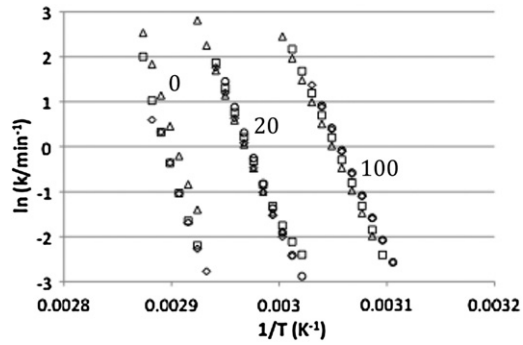

FIGURE 5 Arrhenius plots for the thermal denaturation of rhodopsin in intact disk membranes, in 20 mM, and in 100 mM OG. First-order rate constants were derived from the irreversible denaturation of the protein according to the two-state model. The different symbols used indicate the scan rates of each experiment (*circles*, 0.25 K/min; *diamonds*, 0.5 K/min; *squares*, 1 K/min; *triangles*, 1.5 K/min.)

as the OG concentration increases from 0 to 25 mM. The rhodopsin E_{act} then remains unchanged with further increases in OG concentration. (As discussed previously,

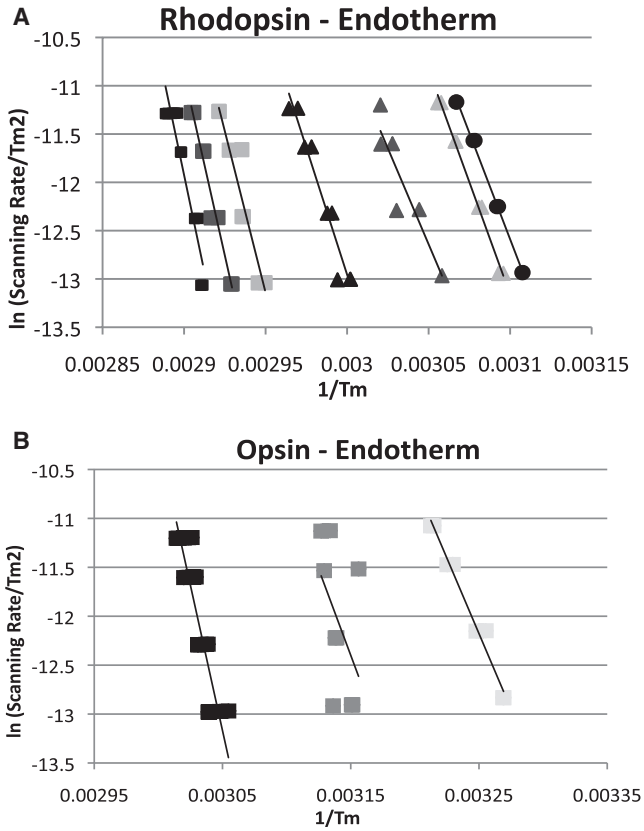

FIGURE 6 (*A*) Plot of ln(scan rate/T_m^2) versus $1/T_m$ for the thermal denaturation of rhodopsin. Rhodopsin T_m was determined at 0 (*black squares*), 5 (*gray squares*), 10 (*light gray squares*), 20 (*black triangles*), 50 (*gray triangles*), 100 (*light gray triangles*), and 200 (*black circles*) mM OG. (*B*) Plot of ln(scan rate/T_m^2) versus $1/T_m$ for the thermal denaturation of opsin. Opsin T_m was determined at 0 (*black squares*), 10 (*gray squares*), and 20 (*light gray squares*) mM OG. Each T_m was determined at scan rates of 1.5, 1.0, 0.5, and 0.25 K/min.

opsin E_{act} cannot be determined by DSC under fully solubilizing conditions due to rapid irreversible denaturation when solubilized.) If the data for rhodopsin E_{act} under subsolubilizing and solubilizing conditions are fitted independently as two straight lines, the lines intersect at ~30 mM OG, the point at which rhodopsin is in mixed micelles with ~30 phospholipids (21). The estimated slope of the line for rhodopsin E_{act} at OG concentrations >30 mM is 0.00359, which is not statistically significantly different from zero ($P = 0.934$). Therefore, reduction of the phospholipid/rhodopsin molar ratio in the micelle to 10 at 100 mM OG and finally to 4 at 200 mM OG had no further effect on E_{act}.

We also calculated E_{act} for rhodopsin in intact, partially solubilized, and fully solubilized disks using an alternate method, which uses the dependence of E_{act} on the height and area of the transition (31) as described in the Methods. This allowed us to verify consistency between the two methods. These data are also shown in Fig. 7.

Rhodopsin thermal denaturation was further investigated using a spectroscopic rather than a calorimetric technique. Rhodopsin exhibits a characteristic absorption maximum at 500 nm due to the bound 11-*cis*-retinal. The loss of this absorption upon thermal denaturation is termed thermal bleaching. The rate of thermal bleaching was determined as a function of temperature for disk membrane samples prepared in an identical manner as for the DSC experiments described previously. Samples were incubated at fixed temperatures that corresponded to the onset and to the completion of thermal denaturation as determined by DSC. The rate of initial thermal bleaching is linear, an example of which is shown in Fig. 8 *A*. The initial rate of thermal bleaching at each temperature in intact disks and at five OG concentrations is shown in Fig. 8 *B*.

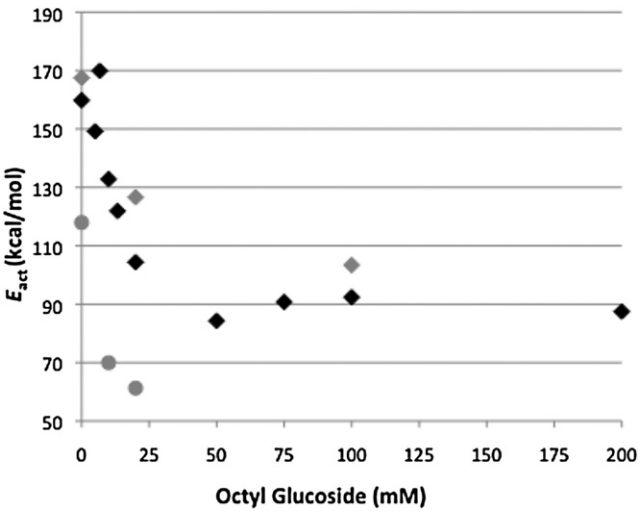

FIGURE 7 E_{act} values (determined from the scan-rate dependence of T_m in Fig. 6) as a function of OG concentration for the thermal denaturation of rhodopsin (*black diamonds*) and opsin (*gray circles*). The E_{act} values determined from the transition peak height and area are also shown at 0, 20, and 100 mM OG (*gray diamonds*).

If rhodopsin thermal bleaching conforms to first-order kinetics the natural log of the concentration should be a linear function of time. The absorbance at 500 nm can be used as a measure of concentration because it is directly proportional to the rhodopsin concentration. As shown in Fig. 8 *C*, the thermal denaturation of rhodopsin is consistent with first-order kinetics in the intact disk membrane as well as at subsolubilizing and fully solubilizing OG concentrations.

The E_{act} of thermal denaturation was determined from the dependence of the rate of thermal bleaching on temperature at each OG concentration using the Arrhenius relationship. This dependence of E_{act} determined from thermal bleaching on the extent of membrane solubilization is shown in Fig. 8 *D*. The calorimetric E_{act} is also shown in Fig. 8 *D* for comparison. The E_{act} of thermal bleaching in disks (OG absent) is consistent with literature values (23). As was found for the E_{act} determined from DSC data, the E_{act} determined from thermal bleaching data decreases dramatically as detergent partitions into the bilayer. At subsolubilizing OG concentrations E_{act} determined from calorimetric data and E_{act} determined from thermal bleaching are not significantly different ($P = 0.453$). Furthermore, above 30 mM OG, the amount of OG is not a statistically significant predictor of E_{act}. That is, the slope of the regression line is not significantly different from zero ($P = 0.225$). Thus, it appears that E_{act} remains constant from 30 mM to 200 mM whether it is determined by calorimetric or by spectroscopic techniques. Although above 30 mM OG, the two E_{act} determinations appear to be statistically different ($P = 0.021$), the important aspect for this study is that further depletion of the phospholipid in the detergent micelle has no effect on E_{act}.

DISCUSSION

The bilayer lipid composition has been shown to be important for the function and stability of membrane proteins (37). However, the mechanism by which the membrane bilayer exerts this stabilizing effect was not clear. Here, we investigated the role of the bilayer in the kinetic stability of rhodopsin. To this end, we built on an earlier study that demonstrated that disruption of the disk membrane bilayer by solubilization in the detergent OG proceeds in a well-defined sequence (21). Rhodopsin thermal denaturation was then examined at different stages in this sequence of disk bilayer solubilization. During the early stages of solubilization the protein exists in a bilayer perturbed by detergent. Upon solubilization the protein exists with phospholipids in a detergent micelle. As more detergent is added, the phospholipids available to interact with the protein in the micelle decrease. These studies indicate that the micellar phospholipids had little or no effect on the stability of rhodopsin.

The effect of perturbing the phospholipid bilayer with OG is immediately apparent in the DSC thermograms as the OG concentration is increased. As OG partitions into the bilayer,

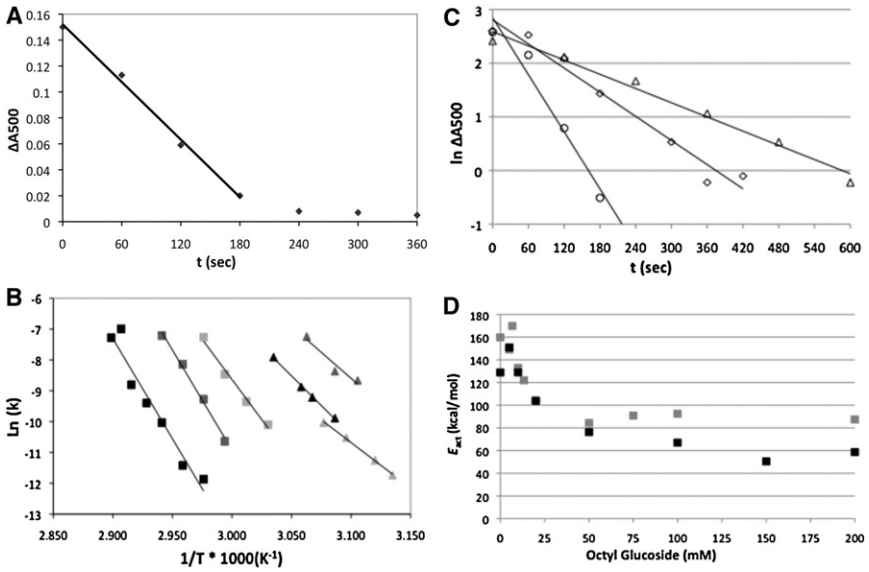

FIGURE 8 (*A*) Loss of absorption at 500 nm (ΔA_{500}) as a function of time. The rate of thermal decay, *k* was calculated from the initial slope. (*B*) Arrhenius plot for the thermal bleaching of rhodopsin determined at concentrations of 0 (*black squares*), 5 (*gray squares*), 10 (*light gray squares*), 20 (*black triangles*), 50 (*gray triangles*), and 100 (*light gray triangles*) mM OG. (*C*) Examples showing first-order nature of thermal bleaching. The ln of ΔA_{500} is plotted against time under the following conditions: 0 mM OG, 344 K (*circles*); 20 mM OG, 336 K (*diamonds*); and 100 mM OG, 324 K (*triangles*). (*D*) The E_{act} as a function of OG concentration for rhodopsin thermal bleaching (*black squares*) are plotted. The E_{act} values determined from scan-rate dependence by DSC (*gray squares*) are shown for comparison.

both rhodopsin and opsin become more vulnerable to thermal denaturation as shown by the decrease in the T_m of the endothermic transition. The transition also broadens as OG partitions into the bilayer. Once the disk membrane was solubilized the ratio of phospholipids/rhodopsin in the mixed micelles continued to decrease from ~30 phospholipids/rhodopsin to ~4 phospholipids/rhodopsin as additional OG was added. However, the T_m of the endothermic rhodopsin transition exhibited only a small decrease with this addition of OG. The slight decrease in T_m may be attributed to the progressive loss of phospholipids that could be interacting with rhodopsin. However, a decrease in the size of the micelle could also affect the rhodopsin transition. Once the rhodopsin was in a micelle the calorimetric transition did not exhibit any additional broadening. These observations suggest that the bilayer structure rather than the phospholipids cosolubilized with rhodopsin stabilize it to thermal denaturation. This is particularly noteworthy because rhodopsin initially cosolubilized with ~30 phospholipids, which is sufficient to form an annular phospholipid layer around the protein (21).

The T_m of protein denaturation and the stability of the protein are intimately related. However, it is important to distinguish its interpretation for kinetically and thermodynamically stable proteins. Very briefly, the T_m of kinetically stable proteins is sensitive to the rate of heating, the scan rate. This dependence of the T_m on the scan rate can be used to determine the E_{act} (15). However, for thermodynamically stabilized proteins the T_m is the temperature at which the protein exists in equilibrium with equal concentrations of native and denatured states. In this case, the thermodynamic parameters can be determined. (For an in-depth discussion of kinetically stable proteins, please see an excellent review by Sanchez-Ruiz (1) and references therein.)

In previous studies we have shown that both opsin and rhodopsin are kinetically stable (12,13). As such, the protein is maintained in its native state due to an energy barrier that inhibits the transition to the denatured state(s) that may be of lower energy than the native state (and thus the native state may not be at an energy minimum). The E_{act} approximates the enthalpic component of this energy barrier. It is important to distinguish this from a thermodynamically stable protein, whose native state is typically governed by a Gibbs free energy minimum. A high energy barrier can protect kinetically stable proteins from sampling conformations that lead to denatured states on a physiologically relevant time scale. However, these proteins will eventually denature in a time-dependent manner (1).

The data presented here demonstrate that the presence of OG in the bilayer significantly lowers the E_{act} of thermal denaturation well before full solubilization of the bilayer regardless of the method used to calculate this value. The E_{act} determined from calorimetry is statistically identical to the E_{act} determined from the rate of thermal bleaching before full solubilization. Both show the same drop in E_{act} as OG partitions into the bilayer. The broadening of the transition as OG partitions into the bilayer likely reflects the decrease in E_{act} of the rhodopsin thermal denaturation as the bilayer becomes saturated with OG. Once the bilayer is destroyed by solubilization there is no further change of the E_{act} determined calorimetrically or of the E_{act} determined from thermal bleaching when the phospholipid/rhodopsin ratio in the mixed micelles is reduced by further addition of OG. This indicates that the phospholipids in the mixed micelle do not contribute to the kinetic stability of rhodopsin even when there are sufficient phospholipids to form an annular layer around the protein. It is likely that the phospholipid-rhodopsin interactions detected by

electron spin resonance (38) and NMR (39) in the intact bilayer are disrupted during the subsolubilizing phase.

It is interesting to compare the magnitude of rhodopsin stabilization by the intact bilayer to rhodopsin stabilization by its chromophore, 11-*cis*-retinal. We have shown that the E_{act} for denaturation of the apoprotein, opsin, is ~100 kcal/mol (12). Thus, the intact bilayer stabilizes rhodopsin to a similar degree as the chromophore. Given the magnitude of the contribution to the kinetic stability by the bilayer and by the chromophore, it is not surprising that solubilized opsin (no bilayer and no chromophore) denatures very readily.

The changes in rhodopsin denaturation properties during solubilization can be directly attributed to documented OG-induced alterations to the disk bilayer. As OG partitions into the membrane bilayer the disorder of the lipid phase increases (29,40). It is likely that the disk membrane also expands with addition of OG because phosphatidylcholine vesicles have been shown to expand when exposed to subsolubilizing levels of OG (29,41). Additionally, it has been reported that the elasticity of a lipid membrane can be altered by OG due to hydrophobic mismatch (42). These observations suggest that conformational restrictions imposed by the bilayer on rhodopsin during thermal denaturation are likely reduced when OG partitions into the bilayer. The data presented here suggest that it is the bilayer matrix that exerts an important stabilizing influence on rhodopsin. This stabilization is likely achieved at least in part by restricting rhodopsin conformational freedom. This is consistent with earlier studies that demonstrated the importance of the dynamics of the hydrocarbon region of the bilayer on rhodopsin conformational changes. In these studies the partial free volume of the bilayer was shown to impact rhodopsin conformational expansion induced upon exposure to light (43–47).

The heat absorbed during the endothermic transition appears unaffected by solubilization. That is, rhodopsin absorbs the same amount of heat regardless of the presence of OG. This suggests that the dominant factor in rhodopsin thermal denaturation is the breakdown of interactions within the protein structure. Because rhodopsin loses little or no α-helical secondary structure upon thermal denaturation (M. Katragadda and A. Albert, unpublished data), these are likely to be hydrogen bonds that form a complex network of helix-helix interactions and between the rhodopsin helices and retinal (48). It is likely that any heat absorption due to disruption of direct protein-lipid interactions are too small to detect in these experiments.

The bilayer plays a complex role in the stability of membrane proteins. This role extends well beyond simply providing a hydrophobic environment. The bilayer is fundamentally a physical matrix that cannot be easily substituted by an alternate structure such as a micelle. It encompasses properties of the bulk lipid matrix as well as specific protein-lipid interactions, both of which are compromised by solubilization. Interestingly, a recent study demonstrated rhodopsin stability in bicelles, structures that mimic the bilayer matrix (49). The stability conferred by the fundamental structure of the bilayer can be adjusted by the bilayer lipid composition. The bilayer lipid composition, especially the presence of cholesterol can alter the T_m and E_{act} of rhodopsin thermal denaturation in reconstituted membranes (50). Furthermore, we have observed that cholesterol in disk membranes altered the rhodopsin T_m (51) and E_{act} (M. Katragadda and A. Albert, unpublished data). However, the magnitude of changing the lipid composition on the E_{act} of rhodopsin thermal denaturation is less than half that observed upon solubilization in OG.

In conclusion, our results indicate that the membrane bilayer stabilizes rhodopsin by increasing the kinetic stability of rhodopsin to thermal denaturation. This kinetic stability may be lowered with addition of detergent because rhodopsin conformation becomes less restricted as the bilayer becomes saturated with detergent. The phospholipids in a micelle do not serve to enhance rhodopsin kinetic stability even if there are a sufficient number to form an annular layer. Therefore, it is likely that the stability is derived at least in part from the structure of the bilayer matrix and that important stabilizing protein-bilayer interactions are not maintained in the micelle structure. These data suggest that the bilayer is designed to increase the kinetic stability of rhodopsin and thus may regulate its lifetime as a functional protein.

The authors thank Professors Philip Yeagle (Rutgers-Newark) for critical reading of the manuscript and Nathan Alder (University of Connecticut) for valuable discussions.

REFERENCES

1. Sanchez-Ruiz, J. M. 2010. Protein kinetic stability. *Biophys. Chem.* 148:1–15.
2. Sanchez-Ruiz, J. M. 1992. Theoretical analysis of Lumry-Eyring models in differential scanning calorimetry. *Biophys. J.* 61:921–935.
3. Plaza del Pino, I. M., B. Ibarra-Molero, and J. M. Sanchez-Ruiz. 2000. Lower kinetic limit to protein thermal stability: a proposal regarding protein stability in vivo and its relation with misfolding diseases. *Proteins.* 40:58–70.
4. Freire, E., W. W. van Osdol, …, J. M. Sanchez-Ruiz. 1990. Calorimetrically determined dynamics of complex unfolding transitions in proteins. *Annu. Rev. Biophys. Biophys. Chem.* 19:159–188.
5. Jaswal, S. S., J. L. Sohl, …, D. A. Agard. 2002. Energetic landscape of alpha-lytic protease optimizes longevity through kinetic stability. *Nature.* 415:343–346.
6. Lee, C., S. H. Park, …, M. H. Yu. 2000. Regulation of protein function by native metastability. *Proc. Natl. Acad. Sci. USA.* 97:7727–7731.
7. Huber, R., and R. W. Carrell. 1989. Implications of the three-dimensional structure of alpha 1-antitrypsin for structure and function of serpins. *Biochemistry.* 28:8951–8966.
8. Carr, C. M., and P. S. Kim. 1993. A spring-loaded mechanism for the conformational change of influenza hemagglutinin. *Cell.* 73:823–832.
9. Bullough, P. A., F. M. Hughson, …, D. C. Wiley. 1994. Structure of influenza haemagglutinin at the pH of membrane fusion. *Nature.* 371:37–43.

10. Chan, D. C., F. Fass, J. M. Berger, and P. S. Kim. 1997. Core structure of gp41 from the HIV envelope glycoprotein. *Cell.* 89:263–273.
11. Orosz, A., J. Wisniewski, and C. Wu. 1996. Regulation of Drosophila heat shock factor trimerization: global sequence requirements and independence of nuclear localization. *Mol. Cell. Biol.* 16:7018–7030.
12. Landin, J. S., M. Katragadda, and A. D. Albert. 2001. Thermal destabilization of rhodopsin and opsin by proteolytic cleavage in bovine rod outer segment disk membranes. *Biochemistry.* 40:11176–11183.
13. Edrington, 5th, T. C., M. Bennett, and A. D. Albert. 2008. Calorimetric studies of bovine rod outer segment disk membranes support a monomeric unit for both rhodopsin and opsin. *Biophys. J.* 95:2859–2866.
14. Morin, P. E., D. Diggs, and E. Freire. 1990. Thermal stability of membrane-reconstituted yeast cytochrome *c* oxidase. *Biochemistry.* 29:781–788.
15. Galisteo, M. L., and J. M. Sanchez-Ruiz. 1993. Kinetic study into the irreversible thermal denaturation of bacteriorhodopsin. *Eur. Biophys. J.* 22:25–30.
16. Epand, R. F., R. M. Epand, and C. Y. Jung. 1999. Glucose-induced thermal stabilization of the native conformation of GLUT 1. *Biochemistry.* 38:454–458.
17. Lepock, J. R., A. M. Rodahl, …, K. H. Cheng. 1990. Thermal denaturation of the Ca2(+)-ATPase of sarcoplasmic reticulum reveals two thermodynamically independent domains. *Biochemistry.* 29:681–689.
18. Merino, J. M., and C. Gutierrez-Merino. 1990. pH and ligand binding modulate the strength of protein–protein interactions in the Ca^{2+}-ATPase from sarcoplasmic reticulum membranes. *Biochim. Biophys. Acta.* 1420:203–213.
19. Zhadan, G. G., C. Cobaleda, …, V. L. Shnyrov. 1997. Protein involvement in thermally induced structural transitions of pig erythrocyte ghosts. *Biochem. Mol. Biol. Int.* 42:11–20.
20. Helenius, A., and K. Simons. 1975. Solubilization of membranes by detergents. *Biochim. Biophys. Acta.* 415:29–79.
21. Stubbs, G. W., and B. J. Litman. 1978. Effect of alterations in the amphipathic microenvironment on the conformational stability of bovine opsin. 1. Mechanism of solubilization of disk membranes by the nonionic detergent, octyl glucoside. *Biochemistry.* 17:215–219.
22. Papermaster, D. S., and W. J. Dreyer. 1974. Rhodopsin content in the outer segment membranes of bovine and frog retinal rods. *Biochemistry.* 13:2438–2444.
23. Hubbard, R. 1958. The thermal stability of rhodopsin and opsin. *J. Gen. Physiol.* 42:259–280.
24. Shnyrov, V. L., and A. L. Berman. 1988. Calorimetric study of thermal denaturation of vertebrate visual pigments. *Biomed. Biochim. Acta.* 47:355–362.
25. Khan, S. M., W. Bolen, …, J. H. McDowell. 1991. Differential scanning calorimetry of bovine rhodopsin in rod-outer-segment disk membranes. *Eur. J. Biochem.* 200:53–59.
26. Albert, A. D., J. E. Young, and P. L. Yeagle. 1996. Rhodopsin-cholesterol interactions in bovine rod outer segment disk membranes. *Biochim. Biophys. Acta.* 1285:47–55.
27. Miljanich, G. P., M. F. Brown, …, J. M. Sturtevant. 1985. Thermotropic behavior of retinal rod membranes and dispersions of extracted phospholipids. *J. Membr. Biol.* 85:79–86.
28. Stubbs, G. W., H. G. Smith, Jr., and B. J. Litman. 1976. Alkyl glucosides as effective solubilizing agents for bovine rhodopsin. A comparison with several commonly used detergents. *Biochim. Biophys. Acta.* 426:46–56.
29. Jackson, M. L., and B. J. Litman. 1982. Rhodopsin-phospholipid reconstitution by dialysis removal of octyl glucoside. *Biochemistry.* 21:5601–5608.
30. Smith, Jr., H. G., G. W. Stubbs, and B. J. Litman. 1975. The isolation and purification of osmotically intact discs from retinal rod outer segments. *Exp. Eye Res.* 20:211–217.
31. Sánchez-Ruiz, J. M., J. L. López-Lacomba, …, P. L. Mateo. 1988. Differential scanning calorimetry of the irreversible thermal denaturation of thermolysin. *Biochemistry.* 27:1648–1652.
32. Rodriguez-Larrea, D., S. Minning, …, J. M. Sanchez-Ruiz. 2006. Role of solvation barriers in protein kinetic stability. *J. Mol. Biol.* 360:715–724.
33. Stubbs, G. W., and B. J. Litman. 1978. Effect of alterations in the amphipathic microenvironment on the conformational stability of bovine opsin. 2. Rate of loss of opsin regenerability. *Biochemistry.* 17:220–225.
34. Shinoda, H., T. Yamaguchi, and R. Hori. 1961. The surface tension and the critical micelle concentration in aqueous solution of β-D-alkyl glucosides and their mixtures. *Bull. Chem. Soc. Jpn.* 34:237–241.
35. Lumry, R., and H. Eyring. 1954. Conformation changes of proteins. *J. Phys. Chem.* 58:110–120.
36. Albert, A. D., K. Boesze-Battaglia, …, R. M. Epand. 1996. Effect of cholesterol on rhodopsin stability in disk membranes. *Biochim. Biophys. Acta.* 1297:77–82.
37. Lee, A. G. 2003. Lipid-protein interactions in biological membranes: a structural perspective. *Biochem. Biophys. Acta.* 1612:1–40.
38. Watts, A., I. D. Volotovski, …, D. Marsh. 1982. Spin-label studies of rhodopsin-lipid interactions. *Biophys. J.* 37:94–95.
39. Albert, A. D., P. Yeagle, and B. J. Litman. 1982. P NMR investigation of rhodopsin-phospholipid interactions in bovine rod outer segment disk membranes. *Biophys. J.* 37:34–36.
40. Wenk, M. R., T. Alt, …, J. Seelig. 1997. Octyl-beta-D-glucopyranoside partitioning into lipid bilayers: thermodynamics of binding and structural changes of the bilayer. *Biophys. J.* 72:1719–1731.
41. Almog, S., B. J. Litman, …, D. Lichtenberg. 1990. States of aggregation and phase transformations in mixtures of phosphatidylcholine and octyl glucoside. *Biochemistry.* 29:4582–4592.
42. Andersen, O. S., and R. E. Koeppe, 2nd. 2007. Bilayer thickness and membrane protein function: an energetic perspective. *Annu. Rev. Biophys. Biomol. Struct.* 36:107–130.
43. Mitchell, D. C., M. Straume, …, B. J. Litman. 1990. Modulation of metarhodopsin formation by cholesterol-induced ordering of bilayer lipids. *Biochemistry.* 29:9143–9149.
44. Straume, M., and B. J. Litman. 1987. Equilibrium and dynamic structure of large, unilamellar, unsaturated acyl chain phosphatidylcholine vesicles. Higher order analysis of 1,6-diphenyl-1,3,5-hexatriene and 1-[4-(trimethylammonio)phenyl]- 6-phenyl-1,3,5-hexatriene anisotropy decay. *Biochemistry.* 26:5113–5120.
45. Straume, M., and B. J. Litman. 1987. Influence of cholesterol on equilibrium and dynamic bilayer structure of unsaturated acyl chain phosphatidylcholine vesicles as determined from higher order analysis of fluorescence anisotropy decay. *Biochemistry.* 26:5121–5126.
46. Straume, M., and B. J. Litman. 1988. Equilibrium and dynamic bilayer structural properties of unsaturated acyl chain phosphatidylcholine-cholesterol-rhodopsin recombinant vesicles and rod outer segment disk membranes as determined from higher order analysis of fluorescence anisotropy decay. *Biochemistry.* 27:7723–7733.
47. Straume, M., D. C. Mitchell, …, B. J. Litman. 1990. Interconversion of metarhodopsins I and II: a branched photointermediate decay model. *Biochemistry.* 29:9135–9142.
48. Sakmar, T. P. 2002. Structure of rhodopsin and the superfamily of seven-helical receptors: the same and not the same. *Curr. Opin. Cell Biol.* 14:189–195.
49. McKibbin, C., N. A. Farmer, …, P. J. Booth. 2007. Opsin stability and folding: modulation by phospholipid bicelles. *J. Mol. Biol.* 374:1319–1332.
50. Bennett, M. P., and D. C. Mitchell. 2008. Regulation of membrane proteins by dietary lipids: effects of cholesterol and docosahexaenoic acid acyl chain-containing phospholipids on rhodopsin stability and function. *Biophys. J.* 95:1206–1216.
51. Albert, A. D., P. L. Yeagle, …, R. Epand. 1994. Effect of cholesterol on retinal rod outer segment disk membranes. *Invest. Ophthalmol. Vis. Sci.* 35:1461.